1521-009X/43/7/1028–1036$25.00
Drug Metabolism and Disposition
U.S. Government work not protected by U.S. copyright

http://dx.doi.org/10.1124/dmd.115.063388
Drug Metab Dispos 43:1028–1036, July 2015

Hepatoselective Nitric Oxide (NO) Donors, V-PYRRO/NO and V-PROLI/NO, in Nonalcoholic Fatty Liver Disease: A Comparison of Antisteatotic Effects with the Biotransformation and Pharmacokinetics

Kamil Kus, Maria Walczak, Edyta Maslak, Agnieszka Zakrzewska, Anna Gonciarz-Dytman, Piotr Zabielski, Barbara Sitek, Krystyna Wandzel, Agnieszka Kij, Adrian Chabowski, Ryan J. Holland, Joseph E. Saavedra, Larry K. Keefer, and Stefan Chlopicki

Jagiellonian Centre for Experimental Therapeutics (K.K., M.W., E.M., A.Z., A.G.-D., B.S., K.W., A.K., S.Ch.), Department of Pharmacokinetics and Physical Pharmacy, Medical College (K.K., M.W., A.G.-D., A.K.), and Department of Experimental Pharmacology, Chair of Pharmacology, Medical College (S.Ch.), Jagiellonian University, Krakow, Poland; Department of Physiology, Medical University of Bialystok, Bialystok, Poland (P.Z., A.Ch.); Leidos Biomedical Research, Inc., Frederick National Laboratory for Cancer Research, Frederick, Maryland (J.E.S.); and Chemical Biology Laboratory, National Cancer Institute, Frederick, Maryland (R.J.H., L.K.K.)

Received January 17, 2015; accepted April 9, 2015

ABSTRACT

V-PYRRO/NO [*O*(2)-vinyl-1-(pyrrolidin-1-yl)diazen-1-ium-1,2-diolate] and V-PROLI/NO (*O*2-vinyl-[2-(carboxylato)pyrrolidin-1-yl]diazen-1-ium-1,2-diolate), two structurally similar diazeniumdiolate derivatives, were designed as liver-selective prodrugs that are metabolized by cytochrome P450 isoenzymes, with subsequent release of nitric oxide (NO). Yet, their efficacy in the treatment of nonalcoholic fatty liver disease (NAFLD) and their comparative pharmacokinetic and metabolic profiles have not been characterized. The aim of the present work was to compare the effects of V-PYRRO/NO and V-PROLI/NO on liver steatosis, glucose tolerance, and liver fatty acid composition in C57BL/6J mice fed a high-fat diet, as well as to comprehensively characterize the ADME (absorption, distribution, metabolism and excretion) profiles of both NO donors. Despite their similar structure, V-PYRRO/NO and V-PROLI/NO showed differences in pharmacological efficacy in the murine model of NAFLD. V-PYRRO/NO, but not V-PROLI/NO, attenuated liver steatosis, improved glucose tolerance, and favorably modified fatty acid composition in the liver. Both compounds were characterized by rapid absorption following i.p. administration, rapid elimination from the body, and incomplete bioavailability. However, V-PYRRO/NO was eliminated mainly by the liver, whereas V-PROLI/NO was excreted mostly in unchanged form by the kidney. V-PYRRO/NO was metabolized by CYP2E1, CYP2C9, CYP1A2, and CYP3A4, whereas V-PROLI/NO was metabolized mainly by CYP1A2. Importantly, V-PYRRO/NO was a better NO releaser in vivo and in the isolated, perfused liver than V-PROLI/NO, an effect compatible with the superior antisteatotic activity of V-PYRRO/NO. In conclusion, V-PYRRO/NO displayed a pronounced antisteatotic effect associated with liver-targeted NO release, whereas V-PROLI/NO showed low effectiveness, was not taken up by the liver, and was eliminated mostly in unchanged form by the kidney.

Introduction

Many commonly used drugs do not possess biologic activity per se, but are metabolized into active metabolites that exert a therapeutic effect. Increasing bioavailability, reducing toxicity, and achieving organ-selective delivery represent the major aims of prodrug development (Han and Amidon, 2000; Huttunen et al., 2008; Testa, 2009). One of the strategies for achieving hepatoselectivity in drugs is to develop prodrugs that are metabolized by specific enzymes in the liver (Han and Amidon, 2000; Erion et al., 2005; Zawilska et al., 2013). Since cytochrome P450–dependent enzymes represent a large family of enzymes responsible for metabolizing a vast number of xenobiotics, and are located mainly in the liver, they constitute an excellent target for liver-specific prodrugs (Huttunen et al., 2008; Ortiz de Montellano, 2013).

V-PYRRO/NO [*O*(2)-vinyl-1-(pyrrolidin-1-yl)diazen-1-ium-1,2-diolate] and V-PROLI/NO (*O*2-vinyl-[2-(carboxylato)pyrrolidin-1-yl]diazen-1-ium-1,2-diolate) (Fig. 1) are both diazeniumdiolates that were designed to deliver nitric oxide (NO) directly to the liver via cytochrome P450–dependent metabolism. The structure of these prodrugs was designed to avoid spontaneous decomposition under physiological conditions and to facilitate cytochrome P450–related biotransformation into their respective epoxides. These unstable intermediates are formed in hepatocytes and hydrolyze, either spontaneously or via enzymatic reaction by hepatic epoxide hydrolase, to generate diazeniumdiolate ions, which spontaneously release

This work was supported by the Polish National Science Center [DEC-2013/11/N/NZ7/00749] and the European Union from the resources of the European Regional Development Fund under the Innovative Economy Programme, grant coordinated by JCET-UJ [POIG.01.01.02-00-069/09].

dx.doi.org/10.1124/dmd.115.063388.

ABBREVIATIONS: AGP, α-acid glycoprotein; AUC, area under the curve; BSA, bovine serum albumin; HFD, high-fat diet; NAFLD, nonalcoholic fatty liver disease; NO, nitric oxide; PUFA, polyunsaturated fatty acids; SFA, saturated fatty acids; TAG, triacylglycerol; V-PROLI/NO, *O*2-vinyl-[2-(carboxylato)pyrrolidin-1-yl]diazen-1-ium-1,2-diolate; V-PYRRO/NO, *O*(2)-vinyl-1-(pyrrolidin-1-yl)diazen-1-ium-1,2-diolate.

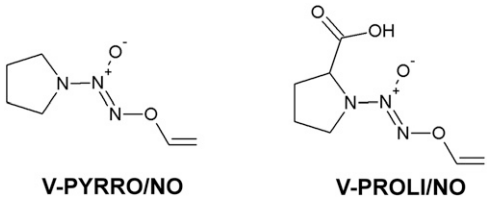

Fig. 1. Structures of V-PYRRO/NO and V-PROLI/NO.

NO (Saavedra et al., 1997). It has been demonstrated that V-PYRRO/NO metabolizes into biologically active NO in isolated hepatocytes but not in liver sinusoidal endothelial cells, Kupffer cells, arterial vascular smooth muscle cells, systemic endothelial cells, or murine macrophages, underscoring the hepatocyte selectivity of NO delivery by V-PYRRO/NO (Saavedra et al., 1997).

In turn, V-PROLI/NO is a novel proline-based analog of V-PYRRO/NO with additional carboxylic acid moiety attached to the molecule to improve the water solubility. Furthermore, the additional functionality makes naturally occurring metabolite *N*-nitrosoproline the major product of decomposition of V-PROLI/NO, resulting in a favorable toxicological profile (Chakrapani et al., 2007; Hong et al., 2010). V-PYRRO/NO, on the other hand, is metabolized to *N*-nitrosopyrrolidine, which is burned with toxicity. To our knowledge, up to now, only one report has demonstrated that V-PROLI/NO is metabolized to NO in human hepatocytes, and in that report, immortalized human HepG2 cells were used (Qu et al., 2009).

In turn, in numerous reports, V-PYRRO/NO has been shown to possess hepatoprotective effects, e.g., in tumor necrosis factor-α –induced hepatitis (Saavedra et al., 1997) or acetaminophen-induced toxicity (Liu et al., 2003), as well as in other in vitro and in vivo models of hepatocyte injury (Kim et al., 2000b; Ricciardi et al., 2001; Liu et al., 2002, 2004, 2005; DeLeve et al., 2003; Li et al., 2003; Gong et al., 2004; Liu and Waalkes, 2005; Qu et al., 2005, 2007; Edwards et al., 2008; Holownia et al., 2009; González et al., 2011; Hu et al., 2013). Moreover, V-PYRRO/NO–derived NO release in the liver was shown to be followed by the elevation of liver cGMP with minimal systemic hypotensive effects (Saavedra et al., 1997). In contrast, hepatoprotective activity by V-PROLI/NO has only been reported in one study, which used the model of arsenic-induced toxicity in human HepG2 cells (Qu et al., 2009).

The evidence shows that NO regulates lipogenesis/lipolysis and controls gluconeogenesis/glycolysis pathways (Duplain et al., 2001; Ijaz et al., 2005; Jobgen et al., 2006). Overexpression of endothelial nitric oxide synthase has consistently been demonstrated to protect against obesity, hyperinsulinemia, adipocyte hypertrophy, decreased plasma triglycerides, and free fatty acid plasma concentration (Sansbury et al., 2012). On the other hand, impaired NO bioavailability has been shown to result in the development of hypertension, insulin resistance, and obesity—being at least in part a consequence of impaired fatty acid oxidation (Duplain et al., 2001; Cook et al., 2003; Le Gouill et al., 2007). Accordingly, liver-selective release of NO could represent an effective novel strategy for preventing nonalcoholic fatty liver disease (NAFLD). The aim of the present study was to compare the therapeutic effects of V-PYRRO/NO and V-PROLI/NO against high-fat diet (HFD)–induced liver steatosis and insulin resistance, as well as to comprehensively characterize the pharmacokinetic and metabolic profiles of these compounds in mice.

Materials and Methods

Chemicals

Chemicals such as high-performance liquid chromatography–grade acetonitrile, formic acid, and methanol were purchased from Merck (Darmstadt, Germany). Ketamine, heparin, and isoflurane were bought from PGF Cefarm (Kraków, Poland). Xylazine, sodium chloride, calcium chloride, magnesium sulfate, sodium bicarbonate, potassium dihydrogen phosphate, glucose, pyruvic acid, EDTA, Tris base, potassium chloride, sucrose, sodium phosphate dibasic, acetone, magnesium chloride, NADPH, Folin & Ciocalteu's phenol reagent, potassium-sodium tartaretetrahydrate, copper sulfate, sodium hydroxide, phenacetin, acetaminophen, tolbutamide, 4-hydroxytolbutamide, bufuralol, 1-hydroxybufuralol, chlorzoxazone, 6-hydroxychlorzoxazone, midazolam, 1-hydroxymidazolam, 4-hydroxymidazolam, dextrorphan, furafylline, sulfaphenazole, (+)-*N*-3-benzylnirvanol, quinidine, disulfiram, and ketoconazole were purchased from Sigma-Aldrich (St. Louis, MO). Water used in the study was prepared using a Milli-Q system (Millipore, Billerica, MA). V-PYRRO/NO and V-PROLI/NO (>99% pure) were synthetized at the Center for Cancer Research at the National Cancer Institute in Frederick, MD, as described previously (Saavedra et al., 1997; Chakrapani et al., 2007).

Animals

Male C57BL/6J mice (16–25 g) and Wistar rats (180–220 g) were purchased from Charles River Laboratories (Raleigh, Germany). Animals were housed in colony cages in a room with constant temperature (21–25°C), a relative humidity of 40–65%, a standard light/dark cycle, and access to food and water ad libitum. Prior to experiments, the animals were fasted overnight with free access to water. All procedures involving animals were conducted according to the Guidelines for Animal Care and Treatment of the European Union and were approved by the Local Ethical Committee for Experiments on Animals at the Jagiellonian University (Krakow, Poland).

Pharmacological Study

Six-week-old, male, C57BL/6J mice were fed a HFD (60 kcal% of fat; (Research Diets, New Brunswick, NJ) for 15 weeks. After 10 weeks of HFD feeding, treatment with V-PYRRO/NO at 5 mg/kg (32 μmol/kg i.p. bolus two times per day) or V-PROLI/NO at 6 mg/kg (29 μmol/kg i.p. bolus two times per day) was carried out for an additional 5 weeks. At the end of the experiment, the animals were anesthetized with ketamine (100 mg/kg, i.p.) and xylazine (10 mg/kg, i.p.).

Glucose Tolerance Test. For the glucose tolerance test, the mice were fasted for 4 hours and then injected intraperitoneally with saturated glucose solution (at 2 g/kg of body weight). Blood was collected from the tail veins prior to glucose administration (0 minute) and at 15, 30, 45, 60, and 120 minutes following administration. Plasma glucose concentrations were measured by the enzymatic photometric method using an automatic biochemical analyzer Pentra 400 (Horiba, Kyoto, Japan) according to the manufacturer's instructions. Area under the curve (AUC) of blood glucose concentration versus time was calculated using the trapezoidal method.

Histologic Evaluation. Liver samples were fixed in 4% buffered formalin. Samples were embedded in OCT (optimal cutting temperature) medium and frozen at −80°C, or prepared according to the standard paraffin method. OCT-embedded 7-μm sections were stained with Oil Red O for fat content examination. Paraffin-embedded 5-μm sections were stained with hematoxylin and eosin for general histology and one-step Gomori's trichrome for fibrosis visualization. Sections were photographed at 100× (Oil Red O) and 200× (H&E, one-step Gomori's trichrome) magnification with an Olympus BX51 light microscope (Olympus Corporation, Tokyo, Japan). Four images of each Oil Red O–stained section (n = 6/group) were analyzed for lipid content using the ImageJ software macro adapted for Oil Red O staining (National Institutes of Health, Bethesda, MD).

Lipid Analysis. Liver samples (ca. 100 mg) were powdered in a mortar precooled with liquid nitrogen followed by extraction of lipids in a chloroform-methanol solution. The fractions of triacylglycerols (TAGs) were separated using thin-layer chromatography, according to the methodology of Baranowski et al. (2013) and Zabielski et al. (2010). Individual fatty acid methyl esters were liberated by acid methanolysis using BF_3MeOH, and were identified and quantified according to the retention times of standards by gas-liquid chromatography (Agilent 5890 Series II gas chromatograph with flame ionization detector, Agilent CP-Sil88 capillary column, 50 m, 0.25-mm i.d., 0.2-μm film; Agilent Technologies, Santa Clara, CA). Total TAG content was estimated as the sum of the particular fatty acid species of the assessed fraction and expressed in nanomoles per gram of tissue. The content of saturated fatty acids (SFA, C14:0, C16:0, C18:0, C20:0, C22:0, C24:0), monounsaturated fatty acids (C16:1, C18:1, C24:1), and polyunsaturated fatty acids

(PUFA, 18:2 *n-6*, 18:3 *n-3*, 20:4 *n-6*, 22:6 *n-3*) in the TAG fractions was analyzed, along with the PUFA/SFA ratio (Wierzbicki et al., 2009).

In Vivo Pharmacokinetics

The 6-week-old male C57BL/6J mice were injected with V-PYRRO/NO or V-PROLI/NO as a single i.v. and i.p. administration at a dose of 5 mg/kg (32 μmol/kg) or 6 mg/kg (29 μmol/kg) for V-PYRRO/NO and V-PROLI/NO, respectively. Animals were anesthetized with isoflurane at a concentration of 3–4% in 100% oxygen and sacrificed at the following time intervals: 0 (before dosing) and 2, 5, 7, 10, 15, 20, 25, 30, 45, 60, 90, 120, and 240 minutes after compound administration. Blood samples were collected into heparinized microfuge tubes and centrifuged at 1000 rpm for 15 minutes. The plasma was separated into clean tubes and frozen at −20°C prior to analysis. The liver tissues were collected and rinsed with phosphate-buffered saline (pH 7.4) and stored at −80°C until analysis.

All data in the pharmacokinetic experiments were processed using Phoenix WinNonlin 6.3 software (Certara, St. Louis, MO). The noncompartmental approach was applied to calculate the basic pharmacokinetic parameters such as mean residence time, AUC, systemic clearance (Cl_T), and volume of distribution at steady state.

Renal Clearance

After a single i.v. injection of V-PYRRO/NO (5 mg/kg) or V-PROLI/NO (6 mg/kg), the 6-week-old mice (n = 7) were individually placed in stainless steel metabolic cages for collection of urine. The urine samples were collected at 0–6, 6–12, and 12–24 hours post dosing. The volumes of the urine samples were recorded, and samples were stored at −20°C until analysis.

Renal elimination was assessed based on the fraction of administered dose excreted in the urine in unchanged form:

$$f_R = \frac{Ae^{\infty}}{D_{iv}} \tag{1}$$

where f_R is the fraction of dose excreted by the kidney, Ae^{∞} is the total amount of studied substance in the urine, and D_{iv} is the administered dose.

Renal clearance (Cl_R) of V-PYRRO/NO and V-PROLI/NO was calculated as follows:

$$Cl_R = f_R \times Cl_T \tag{2}$$

$$Cl_R = \frac{Ae^{\infty}}{AUC_0^{\infty}} \tag{3}$$

Hepatic Extraction Ratio

Hepatic elimination was determined using the ex vivo model of perfused mouse liver. Following i.p. injection of ketamine (100 mg/kg), xylazine (10 mg/kg), and 0.8 mg/kg of heparin, the vena porta and the vena cava inferior were cannulated and ligated, and the liver was perfused using the U-100 system for organ perfusion (Hugo Sachs Elektronik, Harvard Apparatus, March-Hugstetten, Germany) until effluent was blood-free. The liver was than excised and moved to a moist chamber. Perfusion was carried out with Krebs-Hanseleit buffer of the following composition: 118.0 mM NaCl, 2.52 mM $CaCl_2$, 1.16 mM $MgSO_4$, 24.88 mM $NaHCO_3$, 1.18 mM KH_2PO_4, 4.7 mM KCl, 10.0 mM glucose, 2.0 mM pyruvic acid, and 0.5 mM EDTA. After the initial stabilization period (15 minutes), either V-PYRRO/NO or V-PROLI/NO was added at a final concentration of 10 or 50 μM, respectively. The experiments were completed within 1 hour after starting perfusion. The perfusion flow rate was 4.3 ml/min, and samples were collected as follows: inlet samples every 20 minutes, and outlet effluents every 1 minute, between 5 and 20 minutes, and then every 10 minutes. After the experiments, the livers were excised, dried, and weighed.

To ensure the viability of the liver, alanine aminotransferase and lactate dehydrogenase activity in the effluents were measured every 15 minutes for the duration of the experiment by the enzymatic photometric method, using the automatic biochemical analyzer Pentra 400 (Horiba, Kyoto, Japan), according to the manufacturer's instructions.

A control experiment to exclude the binding of V-PYRRO/NO or V-PROLI/NO to the experimental setup was conducted. For this purpose, buffer containing V-PYRRO/NO or V-PROLI/NO was perfused through the perfusion system without mounting of the isolated liver. Buffer samples were collected the same way as in the experiments with the isolated liver.

The hepatic extraction ratio was calculated based on the V-PYRRO/NO and V-PROLI/NO concentrations in the inlet and outlet effluents:

$$E = \frac{C_{in} - C_{out}}{C_{in}} \tag{4}$$

where E is the hepatic extraction ratio and C_{in} and C_{out} are concentrations of studied compounds in inlet or outlet liver effluent.

Protein Binding

Binding of V-PYRRO/NO and V-PROLI/NO to bovine serum albumin (BSA) and α-acid glycoprotein (AGP) was determined using capillary electrophoresis in frontal analysis mode on a Beckman Coulter P/ACE MDQ CE system with a photodiode array detector fixed at 230 nm (Beckman Coulter, Brea, CA). The working conditions were as follows: uncoated fused silica capillary length 60.2 cm (50 cm to the detector) with 50-μm i.d. and 360-μm o.d.; temperature of the capillary 37°C; applied voltage of 15 kV; observed currents of about 56 μA. Following the standard rinsing procedure, the samples were injected at 0.5 psi for 40 seconds (injected sample volume represented 5% of the total capillary volume). The unbound concentrations of V-PYRRO/NO and V-PROLI/NO were determined by comparing the plateau peak height of the equilibrated samples with the peak height of V-PYRRO/NO or V-PROLI/NO in the absence of BSA or AGP.

The results were expressed as the saturation fraction (r), representing the number of moles of compound bound (C_b) per mole of protein (P):

$$r = \frac{C_b}{P} \tag{5}$$

The percentage of binding was determined using eq. 6:

$$\% \text{ bound} = \frac{C_t - C_u}{C_t} \, x \, 100 \tag{6}$$

where C_t is the total concentration of compound in the protein solution, and C_u is the free analyte concentration.

The equilibrium association constant (K_a) in the binding class (m) and the number of binding sites (n) were determined by a nonlinear regression analysis using Wolfram Mathematica 8.0 software (La Jolla, CA) to fit the data to eq. 7:

$$r = \sum_{i=1}^{m} \frac{n_i \cdot C_u}{K_{di} + C_u} \tag{7}$$

where r is the number of moles of drug bound per mole of protein (Cb/Pt, where Pt is the total protein concentration), m is the number of independent classes of binding sites, K_{di} is the dissociation constant for the ith class, and n_i is the number of binding sites in the ith class.

In Vitro Metabolism by Cytochrome P450

Rats were sacrificed by decapitation, and liver microsomes were prepared by differential centrifugation. In brief, liver fragments were washed with 20 mM Tris/KCl buffer (pH 7.4) and homogenized (IKA-Werke GmbH & Co. KG Staufen, Janke, Germany). The homogenate was centrifuged (Sorvall WX Ultra Series; Thermo Scientific, Waltham, MA) at approximately 11,500 × g for 20 minutes at 4°C. The supernatant (S9 fraction) was transferred to new tubes and centrifuged at 100,000 × g for 1 hour at 4°C. The pellet was suspended in 0.15 M KCl and centrifuged again at 100,000 × g for 1 hour at 4°C. The obtained pellet was dispersed in Tris/sucrose buffer and stored at −80°C until use. Protein concentration in the microsomal fraction was determined by Lowry protein assay (Lowry et al., 1951).

V-PYRRO/NO or V-PROLI/NO at a concentration range of 0.5–50 μM was incubated with the rat liver microsomes (1 mg/ml) in 0.1 M phosphate buffer (pH 7.4) containing 10 mM $MgCl_2$. After 5 minutes of preincubation at 37°C, the incubation reactions were initiated with the addition of NADPH to a final concentration of 1 mM and were stopped after 20 minutes by placing samples on ice and adding ice-cold acetonitrile containing internal standard (4-hydroxymephenytoin

at a concentration of 20 ng/ml). Basic kinetic parameters, V_{max} and K_m for V-PYRRO/NO and V-PROLI/NO, were calculated with GraphPad Prism 6.02 software (La Jolla, CA) using nonlinear regression.

To test the involvement of cytochrome P450 isoenzymes in V-PYRRO/NO and V-PROLI/NO metabolism, the following cytochrome P450–dependent isoenzyme inhibitors were used: furafylline (1.5 μg/ml) for CYP1A2, sulfaphenazole (15 μg/ml) for CYP2C9, (+)-*N*-3-benzylnirvanol (1 μg/ml) for CYP2C19, quinidine (15 μg/ml) for CYP2D6, disulfiram (15 μg/ml) for CYP2E1, and ketoconazole (5 μg/ml) for CYP3A4.

To study the effects of V-PYRRO/NO and V-PROLI/NO on cytochrome P450 isoenzyme activity, a "cocktail" method was used based on measurement of the concentration of metabolites derived from cytochrome P450 isoenzyme–specific substrates. In brief, V-PYRRO/NO or V-PROLI/NO, in the concentration range of 0.1 μM to 1 mM, was incubated with rat liver microsomes suspended in 0.1 M phosphate buffer (pH 7.4), 10 mM $MgCl_2$, and substrate cocktail, phenacetin (7.5 μg/ml) for CYP1A2, tolbutamide (2.5 μg/ml) for CYP2C9, bufuralol (12.5 μg/ml) for CYP2D6, chlorzoxazone (12.5 μg/ml) for CYP2E1, and midazolam (7 μg/ml) for CYP3A4. After addition of V-PYRRO/NO or V-PROLI/NO, the reaction mixtures were preincubated for 5 minutes at +37°C in a shaking water bath (Grant Instruments, Royston, UK), and next the reaction was initiated by addition of 1 mM NADPH. Following a 10-minute incubation, the reaction was terminated with an ice-cold mixture of acetonitrile: acetone (1:1; v/v) containing the internal standard dextrorphan (50 ng/ml). Samples were subsequently cooled on ice for 20 minutes to precipitate the protein, and then centrifuged at approximately 15,000 × *g* for 15 minutes at 4°C. The supernatant was analyzed immediately after incubation.

Chromatographic and Mass Spectrometric Analysis

V-PYRRO/NO and V-PROLI/NO concentrations in plasma, liver homogenates, urine, liver effluents, and in the incubation mixture of microsomes (50 μl) were measured after deproteinization using ice-cold acetonitrile (500 μl) containing internal standard (4-hydroxymephenytoin, 20 ng/ml). Samples were subsequently cooled on ice for 20 minutes to precipitate the protein and then centrifuged at approximately 15,000 × *g* for 15 minutes at 4°C. The supernatant was transferred to a high-performance liquid chromatography vial, and 5 μl of supernatant was injected into the analytical column. The analytical system consisted of UFLC Nexera (Shimadzu, Kyoto, Japan) coupled with a QTrap 5500 mass spectrometer (AB Sciex, Framingham, MA). Chromatographic separation was achieved using the Acquity UPLC BEH C18 (1.7 μm, 3.0 × 100 mm; Waters, Milford, MA) analytical column, with acetonitrile and water containing 0.1% formic acid in the isocratic elution (45:55 v/v), at a flow rate of 0.4 ml/min. The analyzed compounds were detected in positive ionization multiple reaction monitoring mode, monitoring the transitions of protonated ions *m/z* 158→70 for V-PYRRO/NO, *m/z* 202→100 for V-PROLI/NO, and *m/z* 235→150 for internal standard. The operating conditions were as follows: curtain gas 20 psi, ion spray voltage 5000 V, temperature 400°C, ion source gases 50 and 15 psi. Nitrogen was used as the curtain and collision gas.

Chromatographic separation of the metabolites of model cytochrome P450 substrates was performed on a Kinetex analytical column (2.6 μm PFP 100 Å, 3 × 100 mm; Phenomenex, Torrance, CA) using an Ultimate 3000 Ultra Performance Liquid Chromatography system (Dionex, Sunnyvale, CA). The mobile phase consisted of acetonitrile containing 0.1% formic acid (eluent A) and water containing 0.1% formic acid (eluent B). At a flow rate of 500 μl/min, the amount of eluent A was increased linearly from 20 to 95% over 2 minutes, maintained at 95% for 6 minutes, returned to 20% over 3 minutes, and left to re-equilibrate for 6 minutes. The total run time was 15 minutes. The analytes were detected using a TSQ Quantum Ultra triple quadrupole mass spectrometer (Thermo Scientific). Heated electrospray ionization was used in both positive and negative mode (for 6-hydroxychlorzoxazone). The selected reaction monitoring transitions for each quantified substance and the internal standard were as follows: acetaminophen *m/z* 152→110, 4-hydroxytolbutamide *m/z* 287→89, 4-hydroxymephenytoin *m/z* 235→150, 1-hydroxybufuralol *m/z* 278→186, 6-hydroxychlorzoxazone *m/z* 184→120, 1-hydroxymidazolam *m/z* 342→324, 4-hydroxymidazolam *m/z* 342→297, and dextrorphan (internal standard) *m/z* 258→157. The operating conditions were as follows: needle voltage 4020 V, vaporizer temperature 250°C, sheath gas (nitrogen) pressure 30 psi, auxiliary gas (nitrogen) pressure 10 psi, and capillary temperature 370°C. The argon gas pressure in the collision cell was approximately 2 mTorr.

Nitrite and Nitrate Measurements

The plasma samples were precipitated with methanol at a ratio of 1:1 (v/v). Liver samples were homogenized with methanol at a ratio of 1:2 (w/v). Following centrifugation at 10,000 × *g* for 10 minutes, 10 μl of supernatant was injected into the separation column.

The concentrations of nitrite and nitrate were measured by ENO-20 system (Eicom, Kyoto, Japan), based on the liquid chromatography method with postcolumn derivatization with Griess reagent. Nitrite and nitrate were separated on a NO-PAK column (4.6 × 50 mm; Eicom). Nitrate was reduced to nitrite by a cadmium-copper column (NO-RED; Eicom). Nitrite was detected based on the Griess reaction, with sulfanilamide and naphthylethylenediamine forming a purple diazo compound with the absorbance of dye product measured at 540 nm. The flow of the mobile phase (carrier solution; Eicom) was 0.33 ml/min. The Griess reagent was delivered at a flow rate of 0.11 ml/min.

Statistical Analysis

Data are expressed as the mean ± S.E.M. The assessment of normality and heterogeneity of variances was performed using the Shapiro-Wilk test and Fligner-Killeen test, respectively. To assess the statistical significance of the pharmacokinetics results, Student's *t* test and the nonparametric Mann-Whitney test were used. For pharmacological experiments, the nonparametric Kruskal-Wallis test or one-way analysis of variance and Tukey's post-hoc test were used. The results were analyzed using Statistica 10.0 software (Statsoft, Tulsa, OK).

Results

Effects of V-PYRRO/NO and V-PROLI/NO Treatment on NAFLD. Treatment with V-PYRRO/NO, but not V-PROLI/NO, attenuated liver steatosis as evidenced by histopathological analysis (Fig. 2, A–C) with semiautomatic quantitative analysis of liver fat content based on Oil Red O–stained slides (Fig. 2D), as well as by liver triglyceride content based on gas chromatography–flame ionization detector chromatography (Fig. 2E). Furthermore, V-PYRRO/NO, but not V-PROLI/NO, favorably changed fatty acid composition by increasing the PUFA/SFA ratio in mice fed a HFD (Fig. 2F). Finally, the overall glucose exposure, calculated on the basis of AUC of blood glucose concentration versus time on the tolerance chart, was significantly improved in V-PYRRO/NO–treated mice, whereas there was no improvement seen in V-PROLI/NO–treated mice (Fig. 2, G and H).

Pharmacokinetic Profile of V-PYRRO/NO and V-PROLI/NO. The mean plasma concentration versus time profiles of V-PYRRO/NO and V-PROLI/NO after i.v. and i.p. administration are depicted in Fig. 3A, and the pharmacokinetic parameters are given in Table 1.

V-PYRRO/NO was eliminated more rapidly than V-PROLI/NO, as evidenced by a lower mean residence time and higher clearance values. V-PYRRO/NO was detectable in plasma for up to 60 minutes after i.v. administration and 30 minutes after i.p. administration, respectively, whereas V-PROLI/NO was measurable over the entire sampling period. Moreover, V-PYRRO/NO was widely distributed in the intra- and extracellular water (Vd_{ss} [steady -state volume of distribution] = 0.88 l/kg), whereas V-PROLI/NO distribution was limited to the extracellular fluid (Vd_{ss} = 0.15 l/kg). In view of the fact that the pharmacological effects were studied following intraperitoneal administration of V-PYRRO/NO and V-PROLI/NO, pharmacokinetic studies following i.p. dosing were also conducted. Both compounds were rapidly absorbed after i.p. administration, with lower bioavailability for V-PYRRO/NO as compared with V-PROLI/NO (about 28 and 51%, respectively). Systemic NO release following i.v. administration of V-PYRRO/NO was higher than with V-PROLI/NO, as evidenced by nitrate and nitrite plasma concentrations (Fig. 3, B and C).

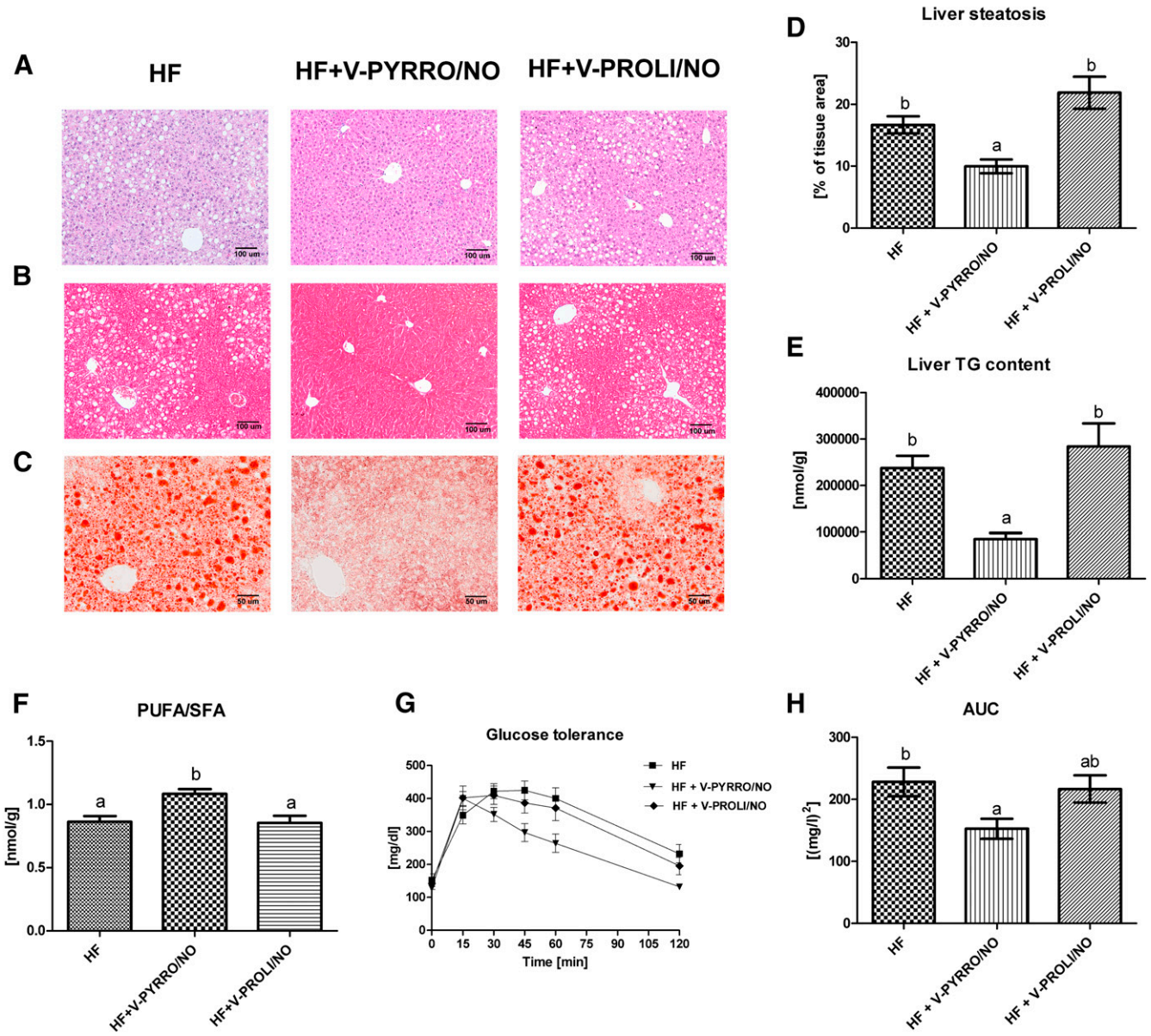

Fig. 2. Representative pictures of liver sections stained with H&E (A), one-step Gomori's trichrome (B), and Oil Red O (C). Liver fat content calculated from Oil Red O pictures (D), liver triglyceride (TG) concentration (E), and PUFA/SFA ratio (F) in the liver of mice. Glucose tolerance curve (G) and AUC of blood glucose concentration versus time (H). Values are the means ± S.E.M. ($n = 6$). Values with different superscript letters within each animal group are significantly different ($P \leq 0.05$). HF, high-fat group; HF+V-PYRRO/NO, high-fat group treated with V-PYRRO/NO; HF+V-PROLI/NO, high-fat group treated with V-PROLI/NO.

Hepatic Metabolism of V-PYRRO/NO and V-PROLI/NO. To assess the liver disposition of V-PYRRO/NO and V-PROLI/NO, the concentration of each compound in liver homogenates was measured following i.v. or i.p. administration of the compounds. V-PYRRO/NO was not detectable, whereas V-PROLI/NO was distributed in the liver with maximum concentrations of 35.8 nmol/g (t_{max} [time to reach the

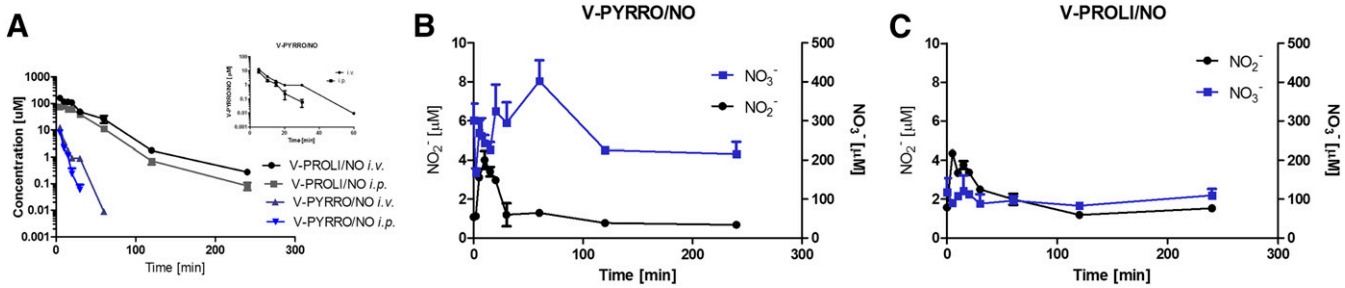

Fig. 3. Comparison of plasma pharmacokinetic profiles of V-PYRRO/NO and V-PROLI/NO after i.v. and i.p. administration in mice (A), and NO_2^-, NO_3^- concentrations in plasma after i.v. administration of each compound (B and C). Values are expressed as the mean ± S.E.M. ($n = 3$ for i.p. and $n = 4$ for i.v. administration).

TABLE 1

Pharmacokinetic parameters of V-PYRRO/NO and V-PROLI/NO after i.v. and i.p. administration in control mice

Parameter	V-PYRRO/NO		V-PROLI/NO	
	Intravenous	Intraperitoneal	Intravenous	Intraperitoneal
C_o (μM)	41.5	—	222.48	—
$AUC_{0\to\infty}$ (μM*min)	218.62	60.9	5669.26	2895.27
MRT (min)	6	7.7	27.87	28.57
C_{max} (μM)	—	7.93	—	79.57
t_{max} (min)	—	5	—	10
V_{ss} (l/kg)	0.88	—	0.149	—
Cl (l/min/kg)	0.146	—	0.0053	—
F (%)	—	27.85	—	51.07

$AUC_{0\to\infty}$, area under the curve extrapolated to infinity; Cl, clearance; C_o, initial concentration; MRT, mean residence time; t_{max}, the time to reach the maximum plasma concentration; V_{ss}, steady-state volume of distribution.

maximal concentration] = 2 minutes) and 23.9 nmol/g (t_{max} = 7 minutes) following i.v. and i.p. administration, respectively. Even after 60 minutes, the concentration of V-PROLI/NO remained elevated (5.3 and 2.5 nmol/g after i.v. and i.p., respectively).

To compare the decomposition of V-PYRRO/NO and V-PROLI/NO in the liver in greater detail, the uptake and metabolism of these analogs were studied in the isolated, perfused mouse liver setup. V-PYRRO/NO exhibited nonspecific binding to the experimental setup, resulting in a 25% decrease in the dose introduced to the liver that was included in the calculations of the hepatic extraction ratio, whereas binding of V-PROLI/NO to the perfusion setup was not significant. As shown in Fig. 4, A and B, the concentrations of V-PYRRO/NO in the liver effluents amounted to about 70% of the initial concentration, taking into account the binding to experimental setup; therefore, the calculated hepatic extraction ratio was about 0.3, and the hepatic clearance was 0.058 l/min/kg. In contrast, V-PROLI/NO was hardly metabolized in the liver, with outflow concentrations of the compound near its inflow concentration. The hepatic extraction ratio for V-PROLI/NO was below 0.1 (about 0.05) and hepatic clearance was 0.0005 ml/min/kg, suggesting negligible liver metabolism of V-PROLI/NO, in contrast with V-PYRRO/NO. These findings were confirmed by the measurements of concentrations of nitrite and nitrate in the liver samples after a 1-hour perfusion of V-PYRRO/NO or V-PROLI/NO at a concentration of 50 μM. V-PYRRO/NO perfusion resulted in elevations in nitrite and nitrate liver content by more than 2-fold (NO_2^-: 4.8 nmol/g; NO_3^-: 23.3 nmol/g), whereas V-PROLI/NO perfusion did not increase nitrite or nitrate concentration in the liver homogenate (NO_2^-: 1.7 nmol/g; NO_3^-: 13.4 nmol/g). Altogether, these results confirm considerable liver metabolism of V-PYRRO/NO, with subsequent NO release, but not of V-PROLI/NO.

Renal Elimination of V-PYRRO/NO and V-PROLI/NO. As shown in Fig. 4C, less than 0.1% of V-PYRRO/NO was eliminated in the urine, whereas approximately 61% of V-PROLI/NO was excreted in the urine as unmodified compound. The calculated renal clearance for V-PYRRO/NO was very low and without physiologic significance, whereas the renal clearance for V-PROLI/NO was significantly higher and amounted to 0.0032 l/min/kg.

Protein Binding of V-PYRRO/NO and V-PROLI/NO. Both analogs bound to BSA with one class of binding site, and the percentage of binding amounted to 25.13 ± 4.5% and 53.33 ± 7.1% for V-PYRRO/NO and V-PROLI/NO, respectively. However, binding affinity to BSA was relatively low (K_a = 1.93 × 10^3 and 7.57 × 10^3 M^{-1} for V-PYRRO/NO and V-PROLI/NO, respectively). Binding of studied analogs to AGP was also very low and not of physiologic significance (3.15 ± 2.9 and 3.05 ± 1.43 for V-PYRRO/NO and V-PROLI/NO, respectively), probably due to the acidic character of these molecules.

Role of Cytochrome P450 in V-PYRRO/NO and V-PROLI/NO Metabolism. The calculated kinetic parameters derived using the Michaelis-Menten transformation (Fig. 5A) for V-PYRRO/NO were K_m = 131.6 ± 38.15 μM and V_{max} = 6.35 ± 1.41 μmol/min/mg protein. Based on the kinetic plots, V-PROLI/NO seems to have a low affinity for the cytochrome P450 isoenzymes. The Eadie-Hofstee plots were nonlinear, suggesting multiple-enzyme catalysis (data not shown).

The effect of selective cytochrome P450 inhibitors on the biotransformation of V-PYRRO/NO and V-PROLI/NO using isoenzyme-selective chemical inhibitors is shown in Fig. 5B. As evidenced by the effects of their respective inhibitors, V-PYRRO/NO was metabolized mainly by CYP2E1, but also by CYP2C9, CYP1A2, and CYP3A4, whereas V-PROLI/NO was biotransformed mainly by CYP1A2 and CYP2C9.

Neither V-PYRRO/NO nor V-PROLI/NO inhibited cytochrome P450 isoenzymes as evidenced by the lack of inhibition of phenacetin-*O*-deethylation (CYP1A2), tolbutamide-4-hydroxylation (CYP2C9), bufuralol-1-hydroxylation (CYP2D6), chlorzoxazone-6-hydroxylation (CYP2E1), and midazolam-1- and -4-hydroxylation (CYP3A4), up to a concentration of 1 mM V-PYRRO/NO and V-PROLI/NO (data not shown).

Discussion

In the present study, we compared two NO donors (V-PYRRO/NO and V-PROLI/NO) that were designed to deliver NO to the liver via cytochrome P450–dependent metabolism by looking at their effects on liver steatosis, liver fatty acid composition, and insulin resistance, and comprehensively analyzing their pharmacokinetics and metabolism profiles. In the study, we demonstrated that, despite having similar chemical structures, only V-PYRRO/NO attenuated liver steatosis, increased the liver PUFA/SFA ratio, and improved postprandial glucose tolerance, whereas V-PROLI/NO was ineffective. Pharmacokinetic studies revealed rapid absorption following i.p. administration,

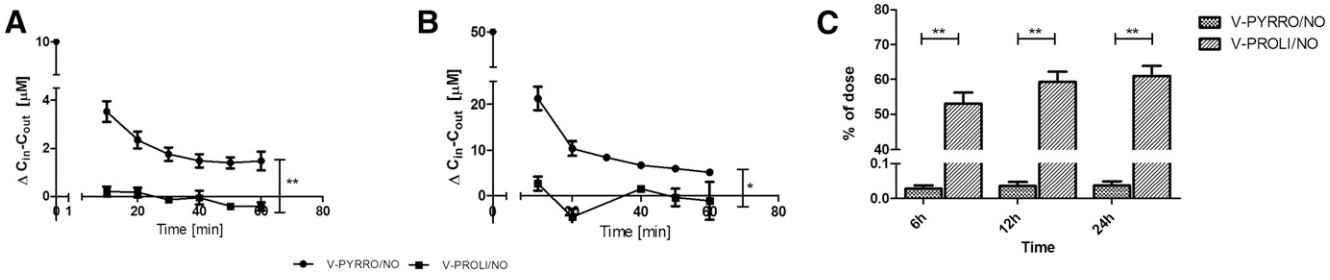

Fig. 4. Calculated differences for V-PYRRO/NO and V-PROLI/NO concentrations between inlet and outlet effluent samples following perfusion with 10 μM (A) and 50 μM compound (B). (C) Fraction of dose that was eliminated unchanged by the kidney. Values are expressed as the mean ± S.E.M. *$P < 0.05$; **$P < 0.01$ (n = 4 for isolated, perfused mouse liver experiments, and n = 7 for renal elimination evaluation).

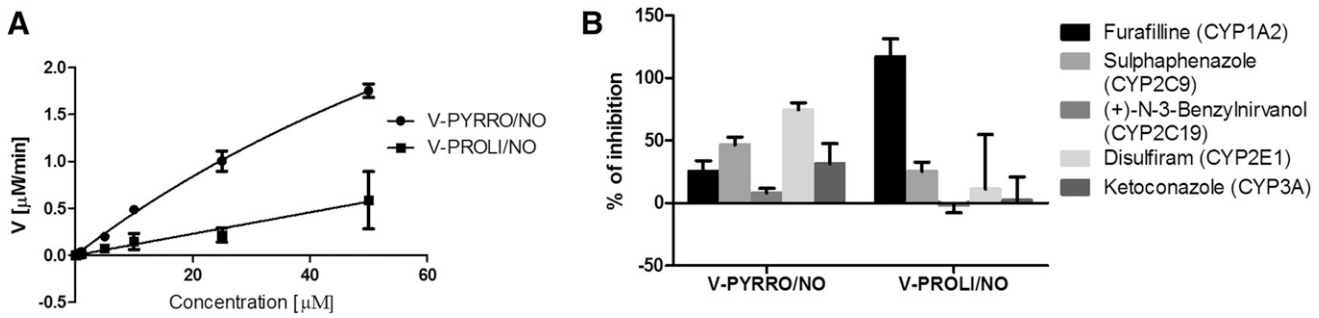

Fig. 5. (A) Michaelis-Menten plots of the enzyme kinetics of V-PYRRO/NO and V-PROLI/NO in rat liver microsomes. (B) The effect of selective cytochrome P450 inhibitors on V-PYRRO/NO and V-PROLI/NO (50 μM) metabolism in rat liver microsomes. Values are shown as the mean percentage ± S.E.M. (n = 3 for furafylline, sulfaphenazole, *N*-benzylnirvanol, and ketoconazole; n = 6 for disulfiram).

intense elimination, and incomplete bioavailability for both V-PYRRO/NO and V-PROLI/NO. However, it was noticed that V-PYRRO/NO was metabolized in the liver by CYP2E1, CYP2C9, and CYP3A4, whereas V-PROLI/NO was eliminated mostly in unchanged form by the kidney. Importantly, V-PYRRO/NO proved to be a better NO releaser in the mouse in vivo and in the isolated liver as compared with V-PROLI/NO. These results were consistent with superior antisteatotic activity for V-PYRRO/NO. In conclusion, we provide clear-cut evidence that V-PYRRO/NO displays a pronounced antisteatotic effect associated with liver-targeted NO release, whereas V-PROLI/NO is not effective, is not taken up by the liver, and is eliminated mostly unchanged by the kidney.

In physiological conditions, NO generated mainly by endothelial nitric oxide synthase (Förstermann and Sessa, 2012) plays a crucial role in liver homeostasis. NO activates soluble guanyl cyclase, which activates cGMP-dependent protein kinase (Pfeifer et al., 2013), and its role is not limited to the regulation of hepatic arterial resistance (Rockey and Shah, 2004). In fact, the NO/cGMP–dependent signaling pathway exerts an anti-inflammatory and antifibrotic effect by limiting Kupffer cell and hepatic stellate cell activation (Tateya et al., 2011). NO also inhibits caspase activation, and therefore apoptosis, in hepatocytes (Kim et al., 2000a). Furthermore, the remarkable regenerative ability of the liver is linked to NO activity (Carnovale and Ronco, 2012). NO also regulates glucose and lipid metabolism (Jobgen et al., 2006), decreases fatty acid storage by improving their catabolism, and attenuates de novo fatty acid synthesis. Moreover, NO regulates glucose metabolism by increasing glucose transport and metabolism as well as inhibiting gluconeogenesis and glycogen deposition (Jobgen et al., 2006).

Clearly, inadequate NO production by liver sinusoidal endothelial cells results in unopposed hepatic stellate cell activation and promotion of liver inflammation, which may contribute to the progression of portal hypertension (Hu et al., 2013), sinusoidal obstruction syndrome (DeLeve, 2008), ischemia-reperfusion injury (Siriussawakul et al., 2010), and liver steatosis (Maslak et al., 2015). In fact, impairment of NO signaling resulted in decreased glucose uptake, fasting hyperglycemia, and the development of insulin resistance (Lutz et al., 2011; An et al., 2012).

In line with the importance of NO in the maintenance of metabolic homeostasis, the beneficial effect of NO-based therapy has been demonstrated in obesity (Jobgen et al., 2009), insulin resistance (Sadri and Lautt, 1999), and liver steatosis (de Oliveira et al., 2006). However, in contrast to the present paper, none of these reports concerned the direct delivery of NO to the liver (Ricardo et al., 2002). In the current study, we aimed at comparing the antisteatotic efficacy of two structurally related hepatocyte-specific NO donors, and revealed a hepatospecific and hepatoprotective action of V-PYRRO/NO, but not of V-PROLI/NO, against NAFLD. Moreover, the liver-specific effects of V-PYRRO/NO–derived NO release not only attenuated liver steatosis, but were also associated with changes in fatty acid composition, in particular the amelioration of the PUFA/SFA ratio, most likely due to inhibition of endogenous fatty acid synthesis. Our findings are of particular importance because fatty acid saturation has been shown to be involved in the pathogenesis of insulin resistance (van den Berg et al., 2010) and metabolic syndrome (Warensjö et al., 2005). In fact, in our previous work, we demonstrated that the effect of V-PYRRO/NO on insulin resistance and steatosis was mediated by NO-dependent Akt activation and inhibition of de novo fatty acid synthesis by Acetyl-CoA carboxylase (ACC) phosphorylation (Maslak et al., 2015). Interestingly, despite previously reported data indicating NO release in vitro (Hong et al., 2010) and favorable toxicity (Chakrapani et al., 2007), V-PROLI/NO did not influence insulin resistance and fatty acid composition in mice in the present study.

The superior pharmacological activity of V-PYRRO/NO was not associated with higher bioavailability than V-PROLI/NO following i.p. administration. In fact, V-PROLI/NO showed greater bioavailability (51%) than V-PYRRO/NO (27%). Similar results for the bioavailability of V-PYRRO/NO were reported by Stinson et al. (2002). The incomplete bioavailability, besides the first-pass effect, might be a result of extrahepatic metabolism of V-PYRRO/NO and V-PROLI/NO, since the cytochrome P450 enzyme system is also located in other extrahepatic tissues, including the lungs, kidneys, and small intestine (Guengerich, 1992; Nebert and Russell, 2002; Ding and Kaminsky, 2003; Paine et al., 2006; Pavek and Dvorak, 2008). Partial decomposition of V-PYRRO/NO and V-PROLI/NO in other organs may explain the increased nitrite and nitrate plasma concentrations detected following i.v. administration of the compounds. However, we are confident that, even though V-PYRRO/NO was partially metabolized in extrahepatic tissues, its pharmacological effect came mostly, if not entirely, from liver-specific NO release.

The results from the specific cytochrome P450 inhibitors demonstrated that V-PYRRO/NO was mainly a substrate for CYP2E1, as well as for CYP1A2, CYP2C9, and CYP3A4, whereas V-PROLI/NO was shown to be metabolized mainly by CYP1A2 and CYP2C9 in the liver. These results are partially in line with the findings of Inami et al. (2006), who showed that CYP2E1, CYP2A6, and CYP2B6 are responsible for V-PYRRO/NO metabolism in human liver microsomes. On the other hand, V-PROLI/NO was metabolized mainly by CYP1A2 and, to a lesser extent, by CYP2E1 and CYP3A4, as reported previously (Chakrapani et al., 2007), but with low enzyme affinity.

Increased metabolism and NO production in V-PROLI/NO–treated HepG2 cells, as compared with V-PYRRO/NO treatment, was previously demonstrated by Hong et al. (2010). However, high concentrations of

V-PYRRO/NO and V-PROLI/NO were required to generate relatively low concentrations of nitrite [reported by Hong et al., 2010 and confirmed by us (unpublished results)], suggesting a relatively low biotransformation of the compounds in HepG2 cells. This notion seems to be in line with recent studies showing that, in human hepatoma cells (e.g., HepG2), the expression of most of cytochrome P450 isoenzymes is substantially reduced as compared with primary human hepatocytes (about 100- to 1000-fold lower) (Westerink and Schoonen, 2007; Pawłowska and Augustin, 2011; Lin et al., 2012). Moreover, in HepG2 cell lines, the activity of cytochrome P450 enzymes is much lower than in ex vivo isolated primary hepatocytes (Westerink and Schoonen, 2007; Lin et al., 2012). Additionally, since the expression and activity of CYP1A2 are higher than those of CYP2E1 in HepG2 cells (Westerink and Schoonen, 2007), Hong et al. (2010) found high release of NO from V-PROLI/NO, as compared with V-PYRRO/NO. In our hands, biotransformation of V-PROLI/NO was dependent on CYP1A2 and CYP2C9, whereas biotransformation of V-PYRRO/NO was mainly dependent on CYP2E1. It is not surprising that Gong et al. (2004) demonstrated that HepG2 cells failed to generate nitrite and nitrate from V-PYRRO/NO. Accordingly, we believe that use of the HepG2 cell line as a model system to study NO release from V-PYRRO/NO and V-PROLI/NO is not relevant to primary hepatocytes or the in vivo setting, thus giving contradictory results from our present study, which was performed in an in vivo and ex vivo isolated liver setup.

In the present work, we also demonstrated that the differences in the plasma pharmacokinetic profiles of V-PYRRO/NO and V-PROLI/NO may be linked to differences in their lipophilicity caused by an additional carboxylic acid moiety in V-PROLI/NO's structure. In silico–predicted log *P* values for both analogs differed from −1.63 to 1.01 for V-PYRRO/NO and from −3.92 to −2.76 for V-PROLI/NO, depending on the pH of the environment. V-PYRRO/NO, being more lipophilic, was widely distributed in the total body water (Vd_{ss} = 0.88 l/kg), whereas V-PROLI/NO distribution was limited only to the extracellular fluid (Vd_{ss} = 0.149 l/kg). Differences in pharmacokinetic profiles can also be related to the participation of proline transporters in the case of V-PROLI/NO, but not of V-PYRRO/NO.

Moreover, the results showed that the affinity of V-PYRRO/NO and V-PROLI/NO to BSA was rather low. V-PROLI/NO was bound to BSA to a greater extent, probably due to the stronger acidic character, which can partially explain its slower elimination and longer biological half-life. Furthermore, we provide evidence that neither compound affects the activity of cytochrome P450, as shown in the direct inhibition study. In summary, both analogs display distinct cytochrome P450 metabolism, distinct pharmacokinetic profile, and differences in renal excretion.

Conclusions

V-PYRRO/NO, but not V-PROLI/NO, protected against high fat diet-induced liver steatosis and improved insulin resistance in mice fed a high-fat diet. The compounds' distinct pharmacological effects can be explained by their pharmacokinetic and metabolic profiles. V-PYRRO/NO displayed a pronounced antisteatotic effect associated with liver-targeted NO release, whereas V-PROLI/NO was ineffective, not taken up by the liver, and was eliminated mostly unchanged by the kidney. It is worth adding that therapy with liver-targeted NO donors, free of systemic hypotensive effects, represents a promising therapeutic strategy not only in NAFLD but also in other liver disorders, such as liver cirrhosis, liver fibrosis, and postischemic injury (Ricciardi et al., 2001; Moal et al., 2002; Edwards et al., 2008) that warrants further studies.

Authorship Contributions

Participated in research design: Kus, Chlopicki.

Conducted experiments: Kus, Walczak, Maslak, Zakrzewska, Gonciarz-Dytman, Zabielski, Sitek, Wandzel, Kij, Chabowski.

Contributed new reagents or analytic tools: Saavedra.

Performed data analysis: Kus, Maslak, Holland, Keefer.

Wrote or contributed to the writing of the manuscript: Kus, Chlopicki, Maslak, Walczak, Holland, Keefer.

References

An Z, Winnick JJ, Moore MC, Farmer B, Smith M, Irimia JM, Roach PJ, and Cherrington AD (2012) A cyclic guanosine monophosphate-dependent pathway can regulate net hepatic glucose uptake in vivo. *Diabetes* **61**:2433–2441.

Baranowski M, Blachnio-Zabielska AU, Zabielski P, Harasim E, Harasiuk D, Chabowski A, and Gorski J (2013) Liver X receptor agonist T0901317 enhanced peroxisome proliferator-activated receptor-delta expression and fatty acid oxidation in rat skeletal muscle. *J Physiol Pharmacol* **64**:289–297.

Carnovale CE and Ronco MT (2012) Role of nitric oxide in liver regeneration. *Ann Hepatol* **11**: 636–647.

Chakrapani H, Showalter BM, Kong L, Keefer LK, and Saavedra JE (2007) V-PROLI/NO, a prodrug of the nitric oxide donor, PROLI/NO. *Org Lett* **9**:3409–3412.

Cook S, Hugli O, Egli M, Vollenweider P, Burcelin R, Nicod P, Thorens B, and Scherrer U (2003) Clustering of cardiovascular risk factors mimicking the human metabolic syndrome X in eNOS null mice. *Swiss Med Wkly* **133**:360–363.

Deleve LD (2008) Sinusoidal obstruction syndrome. *Gastroenterol Hepatol (N Y)* **4**:101–103.

DeLeve LD, Wang X, Kanel GC, Ito Y, Bethea NW, McCuskey MK, Tokes ZA, Tsai J, and McCuskey RS (2003) Decreased hepatic nitric oxide production contributes to the development of rat sinusoidal obstruction syndrome. *Hepatology* **38**:900–908.

de Oliveira CPMS, Simplicio FI, de Lima VMR, Yuahasi K, Lopasso FP, Alves VAF, Abdalla DSP, Carrilho FJ, Laurindo FRM, and de Oliveira MG (2006) Oral administration of S-nitroso-N-acetylcysteine prevents the onset of non alcoholic fatty liver disease in rats. *World J Gastroenterol* **12**:1905–1911.

Ding X and Kaminsky LS (2003) Human extrahepatic cytochromes P450: function in xenobiotic metabolism and tissue-selective chemical toxicity in the respiratory and gastrointestinal tracts. *Annu Rev Pharmacol Toxicol* **43**:149–173.

Duplain H, Burcelin R, Sartori C, Cook S, Egli M, Lepori M, Vollenweider P, Pedrazzini T, Nicod P, and Thorens B, et al. (2001) Insulin resistance, hyperlipidemia, and hypertension in mice lacking endothelial nitric oxide synthase. *Circulation* **104**:342–345.

Edwards C, Feng H-Q, Reynolds C, Mao L, and Rockey DC (2008) Effect of the nitric oxide donor V-PYRRO/NO on portal pressure and sinusoidal dynamics in normal and cirrhotic mice. *Am J Physiol Gastrointest Liver Physiol* **294**:G1311–G1317.

Erion MD, van Poelje PD, Mackenna DA, Colby TJ, Montag AC, Fujitaki JM, Linemeyer DL, and Bullough DA (2005) Liver-targeted drug delivery using HepDirect prodrugs. *J Pharmacol Exp Ther* **312**:554–560.

Förstermann U and Sessa WC (2012) Nitric oxide synthases: regulation and function. *Eur Heart J* **33**:829–837, 837a–837d.

Gong P, Cederbaum AI, and Nieto N (2004) The liver-selective nitric oxide donor O2-vinyl 1-(pyrrolidin-1-yl)diazen-1-ium-1,2-diolate (V-PYRRO/NO) protects HepG2 cells against cytochrome P450 2E1-dependent toxicity. *Mol Pharmacol* **65**:130–138.

González R, Cruz A, Ferrín G, López-Cillero P, Fernández-Rodríguez R, Briceño J, Gómez MA, Rufián S, Mata MdeL, and Martínez-Ruiz A, et al. (2011) Nitric oxide mimics transcriptional and post-translational regulation during α-tocopherol cytoprotection against glycochenodeoxycholate-induced cell death in hepatocytes. *J Hepatol* **55**:133–144.

Guengerich FP (1992) Characterization of human cytochrome P450 enzymes. *FASEB J* **6**:745–748.

Han HK and Amidon GL (2000) Targeted prodrug design to optimize drug delivery. *AAPS PharmSci* **2**:E6.

Holownia A, Jablonski J, Skiepko A, Mroz R, Sitko E, and Braszko JJ (2009) Ruthenium red protects HepG2 cells overexpressing CYP2E1 against acetaminophen cytotoxicity. *Naunyn Schmiedebergs Arch Pharmacol* **379**:27–35.

Hong SY, Borchert GL, Maciag AE, Nandurdikar RS, Saavedra JE, Keefer LK, Phang JM, and Chakrapani H (2010) The Nitric Oxide Prodrug V-PROLI/NO Inhibits Cellular Uptake of Proline. *ACS Med Chem Lett* **1**:386–389.

Hu LS, George J, and Wang JH (2013) Current concepts on the role of nitric oxide in portal hypertension. *World J Gastroenterol* **19**:1707–1717.

Huttunen KM, Mähönen N, Raunio H, and Rautio J (2008) Cytochrome P450-activated prodrugs: targeted drug delivery. *Curr Med Chem* **15**:2346–2365.

Ijaz S, Yang W, Winslet MC, and Seifalian AM (2005) The role of nitric oxide in the modulation of hepatic microcirculation and tissue oxygenation in an experimental model of hepatic steatosis. *Microvasc Res* **70**:129–136.

Inami K, Nims RW, Srinivasan A, Citro ML, Saavedra JE, Cederbaum AI, and Keefer LK (2006) Metabolism of a liver-selective nitric oxide-releasing agent, V-PYRRO/NO, by human microsomal cytochromes P450. *Nitric Oxide* **14**:309–315.

Jobgen W, Meininger CJ, Jobgen SC, Li P, Lee M-J, Smith SB, Spencer TE, Fried SK, and Wu G (2009) Dietary L-arginine supplementation reduces white fat gain and enhances skeletal muscle and brown fat masses in diet-induced obese rats. *J Nutr* **139**:230–237.

Jobgen WS, Fried SK, Fu WJ, Meininger CJ, and Wu G (2006) Regulatory role for the arginine-nitric oxide pathway in metabolism of energy substrates. *J Nutr Biochem* **17**:571–588.

Kim YM, Chung HT, Simmons RL, and Billiar TR (2000a) Cellular non-heme iron content is a determinant of nitric oxide-mediated apoptosis, necrosis, and caspase inhibition. *J Biol Chem* **275**:10954–10961.

Kim YM, Kim TH, Chung HT, Talanian RV, Yin XM, and Billiar TR (2000b) Nitric oxide prevents tumor necrosis factor alpha-induced rat hepatocyte apoptosis by the interruption of mitochondrial apoptotic signaling through S-nitrosylation of caspase-8. *Hepatology* **32**:770–778.

Le Gouill E, Jimenez M, Binnert C, Jayet PY, Thalmann S, Nicod P, Scherrer U, and Vollenweider P (2007) Endothelial nitric oxide synthase (eNOS) knockout mice have defective mitochondrial beta-oxidation. *Diabetes* **56**:2690–2696.

Li C, Liu J, Saavedra JE, Keefer LK, and Waalkes MP (2003) The nitric oxide donor, V-PYRRO/NO, protects against acetaminophen-induced nephrotoxicity in mice. *Toxicology* **189**:173–180.
Lin J, Schyschka L, Mühl-Benninghaus R, Neumann J, Hao L, Nussler N, Dooley S, Liu L, Stöckle U, and Nussler AK, et al. (2012) Comparative analysis of phase I and II enzyme activities in 5 hepatic cell lines identifies Huh-7 and HCC-T cells with the highest potential to study drug metabolism. *Arch Toxicol* **86**:87–95.
Liu J, He Y-Y, Chignell CF, Clark J, Myers P, Saavedra JE, and Waalkes MP (2005) Limited protective role of V-PYRRO/NO against cholestasis produced by alpha-naphthylisothiocyanate in mice. *Biochem Pharmacol* **70**:144–151.
Liu J, Li C, Waalkes MP, Clark J, Myers P, Saavedra JE, and Keefer LK (2003) The nitric oxide donor, V-PYRRO/NO, protects against acetaminophen-induced hepatotoxicity in mice. *Hepatology* **37**:324–333.
Liu J, Qu W, Saavedra JE, and Waalkes MP (2004) The nitric oxide donor, O2-vinyl 1-(pyrrolidin-1-yl)diazen-1-ium-1,2-diolate (V-PYRRO/NO), protects against cadmium-induced hepatotoxicity in mice. *J Pharmacol Exp Ther* **310**:18–24.
Liu J, Saavedra JE, Lu T, Song J-G, Clark J, Waalkes MP, and Keefer LK (2002) O(2)-Vinyl 1-(pyrrolidin-1-yl)diazen-1-ium-1,2-diolate protection against D-galactosamine/endotoxin-induced hepatotoxicity in mice: genomic analysis using microarrays. *J Pharmacol Exp Ther* **300**:18–25.
Liu J and Waalkes MP (2005) Nitric oxide and chemically induced hepatotoxicity: beneficial effects of the liver-selective nitric oxide donor, V-PYRRO/NO. *Toxicology* **208**:289–297.
Lowry OH, Rosebrough NJ, Farr AL, and Randall RJ (1951) Protein measurement with the Folin phenol reagent. *J Biol Chem* **193**:265–275.
Lutz SZ, Hennige AM, Feil S, Peter A, Gerling A, Machann J, Kröber SM, Rath M, Schürmann A, and Weigert C, et al. (2011) Genetic ablation of cGMP-dependent protein kinase type I causes liver inflammation and fasting hyperglycemia. *Diabetes* **60**:1566–1576.
Maslak E, Zabielski P, Kochan K, Kus K, Jasztal A, Sitek B, Proniewski B, Wojcik T, Gula K, and Kij A, et al. (2015) The liver-selective NO donor, V-PYRRO/NO, protects against liver steatosis and improves postprandial glucose tolerance in mice fed high fat diet. *Biochem Pharmacol* **93**:389–400.
Moal F, Chappard D, Wang J, Vuillemin E, Michalak-Provost S, Rousselet MC, Oberti F, Calès P (2002) Fractal dimension can distinguish models and pharmacologic changes in liver fibrosis in rats. *Hepatology* **36**(4 Pt 1), 840–9.
Nebert DW and Russell DW (2002) Clinical importance of the cytochromes P450. *Lancet* **360**: 1155–1162.
Ortiz de Montellano PR (2013) Cytochrome P450-activated prodrugs. *Future Med Chem* **5**: 213–228.
Paine MF, Hart HL, Ludington SS, Haining RL, Rettie AE, and Zeldin DC (2006) The human intestinal cytochrome P450 "pie". *Drug Metab Dispos* **34**:880–886.
Pavek P and Dvorak Z (2008) Xenobiotic-induced transcriptional regulation of xenobiotic metabolizing enzymes of the cytochrome P450 superfamily in human extrahepatic tissues. *Curr Drug Metab* **9**:129–143.
Pawłowska M and Augustin E (2011) Expression systems of cytochrome P450 proteins in studies of drug metabolism in vitro. *Postepy Hig Med Dosw* **65**:367–376.
Pfeifer A, Kilić A, and Hoffmann LS (2013) Regulation of metabolism by cGMP. *Pharmacol Ther* **140**:81–91.
Qu W, Liu J, Dill AL, Saavedra JE, Keefer LK, and Waalkes MP (2009) V-PROLI/NO, a nitric oxide donor prodrug, protects liver cells from arsenic-induced toxicity. *Cancer Sci* **100**: 382–388.
Qu W, Liu J, Fuquay R, Saavedra JE, Keefer LK, and Waalkes MP (2007) The nitric oxide prodrug, V-PYRRO/NO, mitigates arsenic-induced liver cell toxicity and apoptosis. *Cancer Lett* **256**:238–245.
Qu W, Liu J, Fuquay R, Shimoda R, Sakurai T, Saavedra JE, Keefer LK, and Waalkes MP (2005) The nitric oxide prodrug, V-PYRRO/NO, protects against cadmium toxicity and apoptosis at the cellular level. *Nitric Oxide* **12**:114–120.
Ricardo KFS, Shishido SM, de Oliveira MG, and Krieger MH (2002) Characterization of the hypotensive effect of S-nitroso-N-acetylcysteine in normotensive and hypertensive conscious rats. *Nitric Oxide* **7**:57–66.
Ricciardi R, Foley DP, Quarfordt SH, Saavedra JE, Keefer LK, Wheeler SM, Donohue SE, Callery MP, and Meyers WC (2001) V-PYRRO/NO: an hepato-selective nitric oxide donor improves porcine liver hemodynamics and function after ischemia reperfusion. *Transplantation* **71**:193–198.
Rockey DC and Shah V (2004) Nitric oxide biology and the liver: report of an AASLD research workshop. *Hepatology* **39**:250–257.
Saavedra JE, Billiar TR, Williams DL, Kim YM, Watkins SC, and Keefer LK (1997) Targeting nitric oxide (NO) delivery in vivo. Design of a liver-selective NO donor prodrug that blocks tumor necrosis factor-alpha-induced apoptosis and toxicity in the liver. *J Med Chem* **40**:1947–1954.
Sadri P and Lautt WW (1999) Blockade of hepatic nitric oxide synthase causes insulin resistance. *Am J Physiol* **277**:G101–G108.
Sansbury BE, Cummins TD, Tang Y, Hellmann J, Holden CR, Harbeson MA, Chen Y, Patel RP, Spite M, and Bhatnagar A, et al. (2012) Overexpression of endothelial nitric oxide synthase prevents diet-induced obesity and regulates adipocyte phenotype. *Circ Res* **111**:1176–1189.
Siriussawakul A, Zaky A, and Lang JD (2010) Role of nitric oxide in hepatic ischemia-reperfusion injury. *World J Gastroenterol* **16**:6079–6086.
Stinson SF, House T, Bramhall C, Saavedra JE, Keefer LK, and Nims RW (2002) Plasma pharmacokinetics of a liver-selective nitric oxide-donating diazeniumdiolate in the male C57BL/6 mouse. *Xenobiotica* **32**:339–347.
Tateya S, Rizzo NO, Handa P, Cheng AM, Morgan-Stevenson V, Daum G, Clowes AW, Morton GJ, Schwartz MW, and Kim F (2011) Endothelial NO/cGMP/VASP signaling attenuates Kupffer cell activation and hepatic insulin resistance induced by high-fat feeding. *Diabetes* **60**:2792–2801.
Testa B (2009) Prodrugs: bridging pharmacodynamic/pharmacokinetic gaps. *Curr Opin Chem Biol* **13**:338–344.
van den Berg SA, Guigas B, Bijland S, Ouwens M, Voshol PJ, Frants RR, Havekes LM, Romijn JA, and van Dijk KW (2010) High levels of dietary stearate promote adiposity and deteriorate hepatic insulin sensitivity. *Nutr Metab (Lond)* **7**:24.
Warensjö E, Risérus U, and Vessby B (2005) Fatty acid composition of serum lipids predicts the development of the metabolic syndrome in men. *Diabetologia* **48**:1999–2005.
Westerink WMA and Schoonen WGEJ (2007) Cytochrome P450 enzyme levels in HepG2 cells and cryopreserved primary human hepatocytes and their induction in HepG2 cells. *Toxicol In Vitro* **21**:1581–1591.
Wierzbicki M, Chabowski A, Zendzian-Piotrowska M, Harasim E, and Górski J (2009) Chronic, in vivo, PPARalpha activation prevents lipid overload in rat liver induced by high fat feeding. *Adv Med Sci* **54**:59–65.
Zabielski P, Baranowski M, Błachnio-Zabielska A, Zendzian-Piotrowska M, and Górski J (2010) The effect of high-fat diet on the sphingolipid pathway of signal transduction in regenerating rat liver. *Prostaglandins Other Lipid Mediat* **93**:75–83.
Zawilska JB, Wojcieszak J, and Olejniczak AB (2013) Prodrugs: a challenge for the drug development. *Pharmacol Rep* **65**:1–14.

Address correspondence to: Stefan Chlopicki, Jagiellonian Centre for Experimental Therapeutics (JCET), Jagiellonian University. Bobrzynskiego 14, 30-348 Krakow, Poland. E-mail: stefan.chlopicki@jcet.eu